Superhydrophobic and superelastic conductive rubber composite for wearable strain sensors with ultrahigh sensitivity and excellent anti-corrosion property

Ling Wang [a], Xuewu Huang [a], Hao Wang [a], Xin Song [a], Mingjun Hu [b], Long-Cheng Tang [c], Jiefeng Gao*[a]

[a] School of Chemistry and Chemical Engineering, Yangzhou University, Yangzhou, Jiangsu, 225002, China

[b] School of Materials Science and Engineering, Beihang University, Beijing, China.

[c] Key Laboratory of Organosilicon Chemistry and Material Technology of Ministry of Education, College of Material, Chemistry and Chemical Engineering, Hangzhou Normal University, Hangzhou 311121, China

*Corresponding authors: jfgao@yzu.edu.cn;

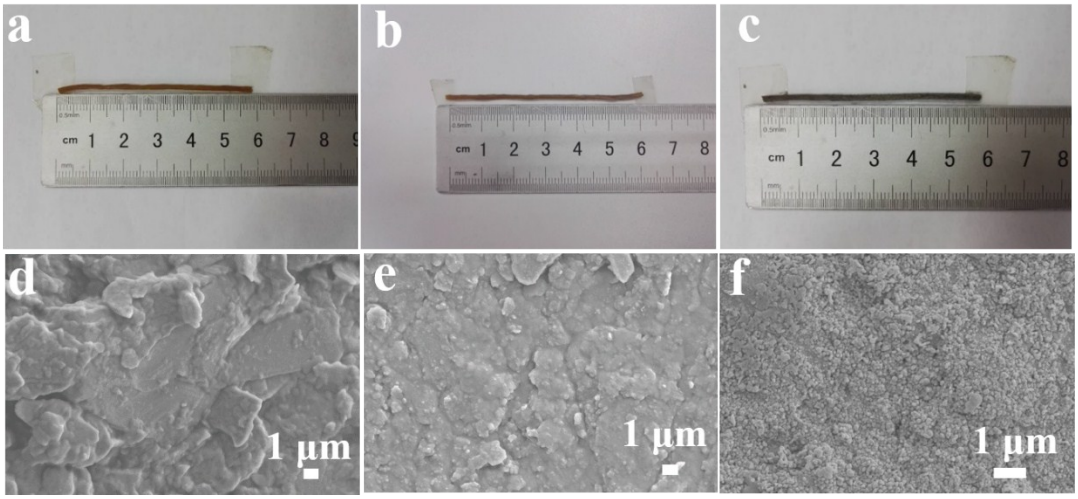

Fig. S1 Photograph for (a) the pristine RB with a yellow color. (b) PDA modified RB and (c) RB/PDA/AgNPs-90. SEM image of the surface morphology for (d) the pristine RB. (e) RB/PDA. and (f) RB/PDA/AgNPs-90.

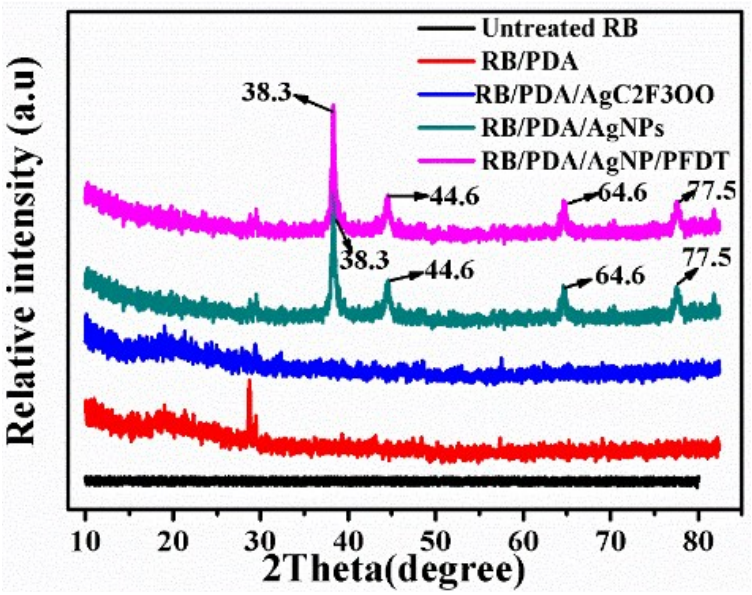

Fig. S2 XRD patterns for different RB based composite.

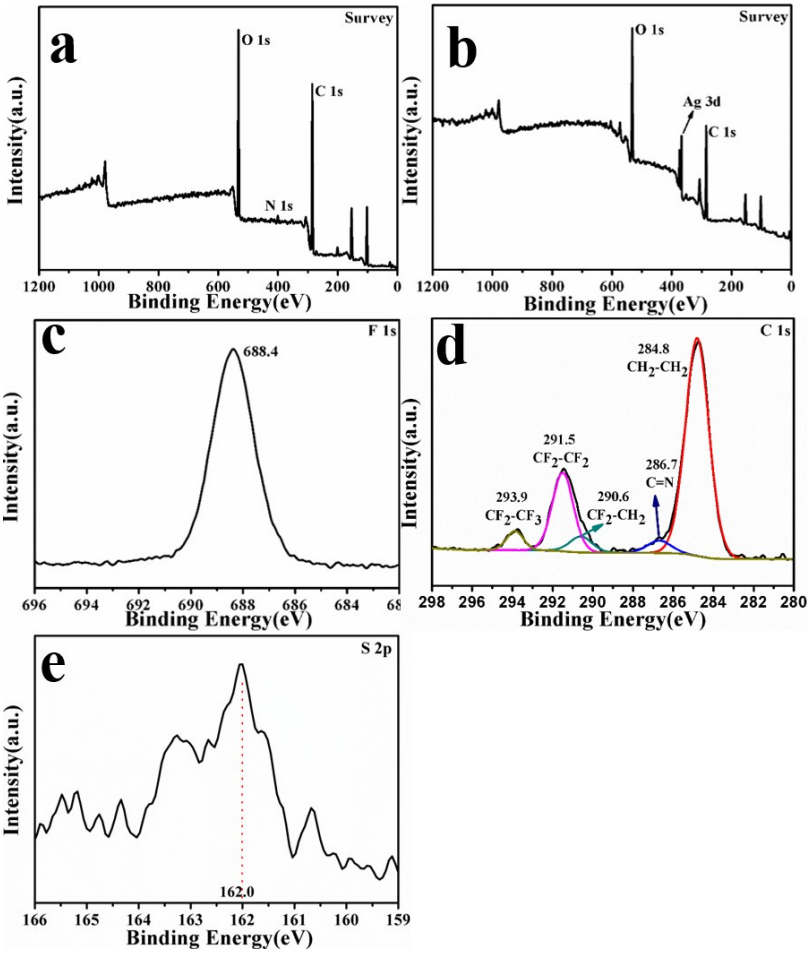

Fig. S3 (a) Survey spectrum of the surface of RB/PDA. (b) Survey spectrum of RB/PDA/AgNPs-90. (c) F1s peak of the RB/PDA/AgNPs-90/PFDT. (d) Resolved C1s peaks of the RB/PDA/AgNPs-90/PFDT. (e) S2p peak of the RB/PDA/AgNPs-90/PFDT

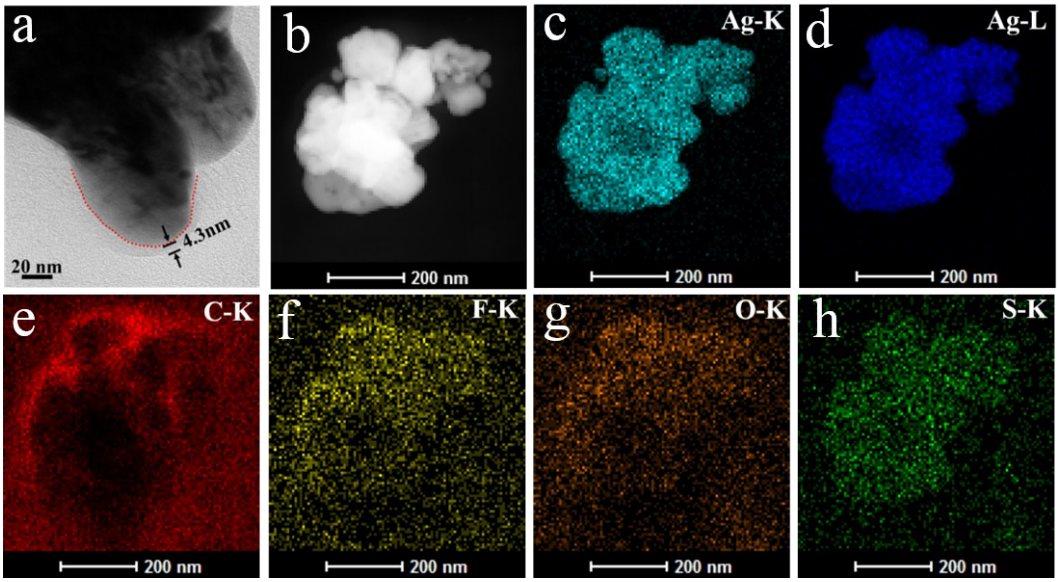

Fig. S4 (a) HRTEM images of AgNPs peeled off from the CPC based strain sensor. (a thin layer coating of PFDT with the thickness of about 4.3 nm can be observed). (b) The AgNP aggregate used for elemental mapping. (c-h) Scanning mapping images of (b) for Ag, C, F, O, S, respectively.

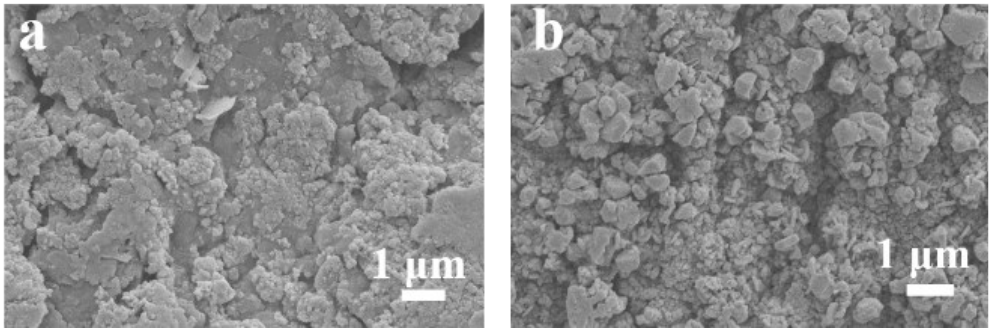

Fig. S5 The morphology of RB/PDA/AgNPs-10 (a) and RB/PDA/AgNPs-120 (b).

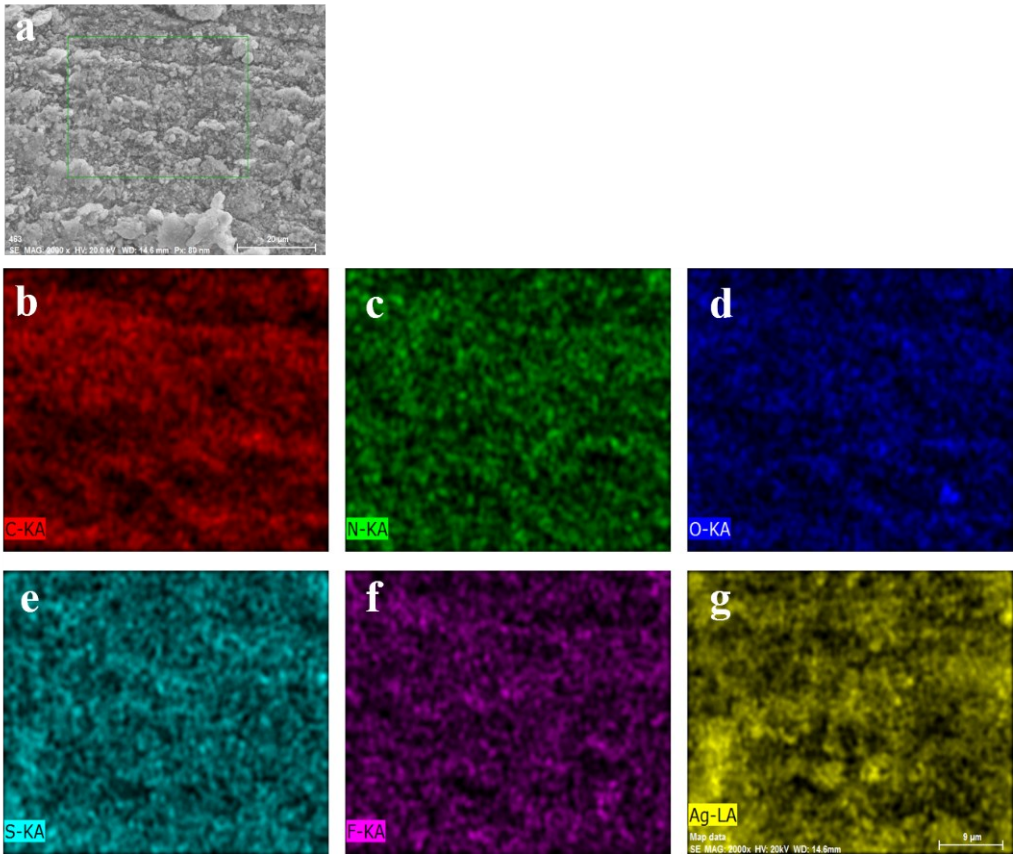

Fig. S6 (a) The SEM image of RB/PDA/AgNPs-90/PFDT for elemental analysis. (b-g) Scanning mapping images of the green area in (a) for C, N, O, S, F, Ag respectively.

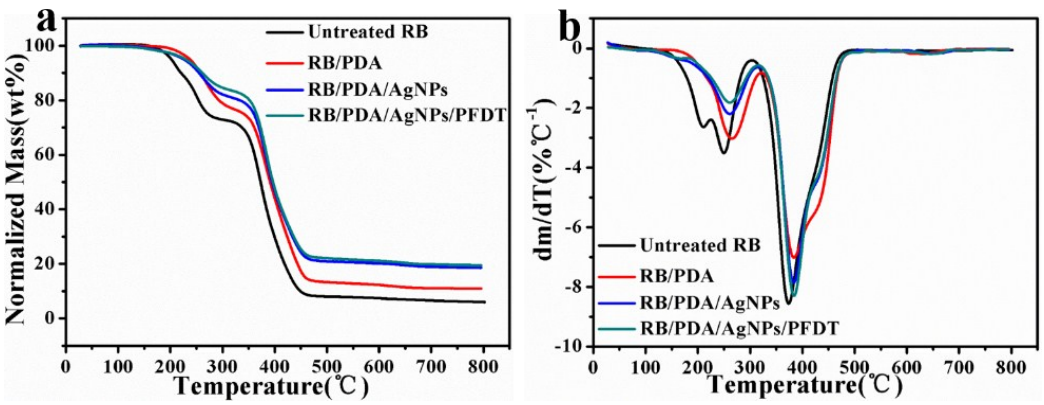

Fig. S7 (a) TGA and (b) DTG curves for RB basd composites.

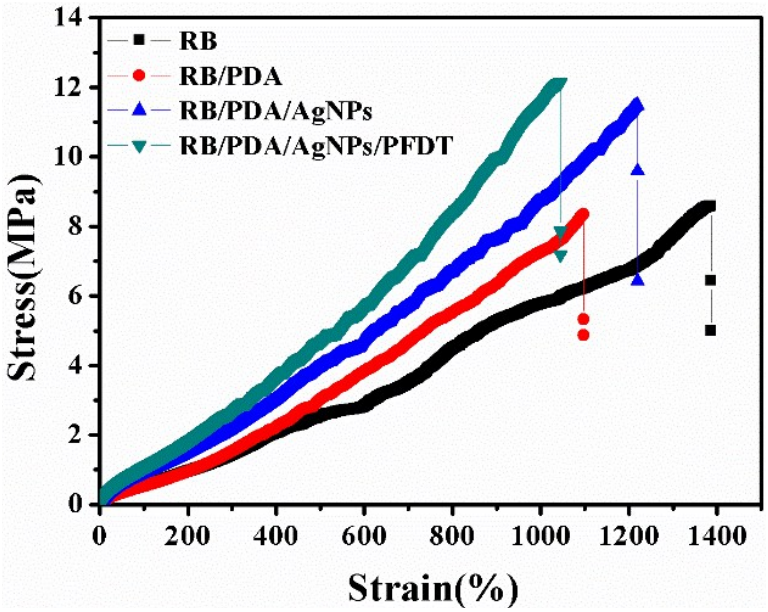

Fig. S8 Stress-strain curves for different RB based composites.

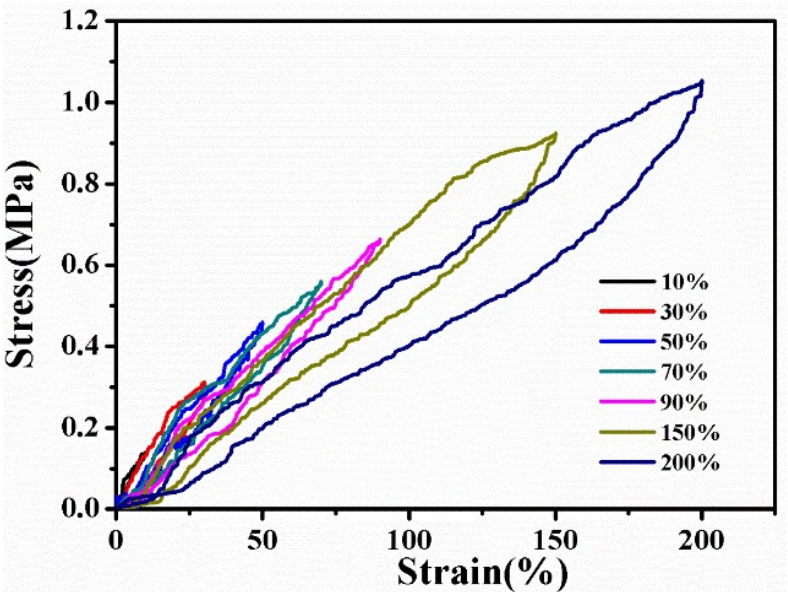

Fig. S9 The cyclic stress-strain curves for RB/PDA/AgNPs-90/PFDT under different applied strain.

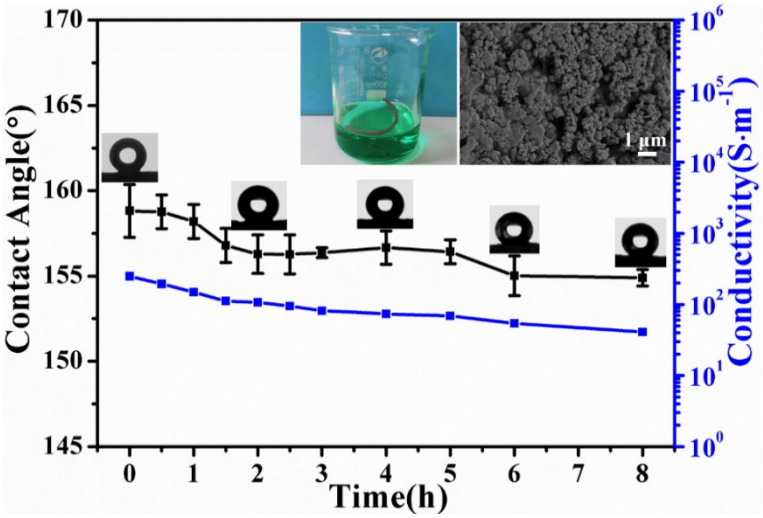

Fig. S10 The CA and electrical conductivity variation of the RB/PDA/AgNPs-90/PFDT placed into the acid solution (pH=1) as the immersion time (Insets are photograph of the superhydrophobic RB composite placed in the acid solution and the SEM image of the surface of the composite in the acid solution for 8h)

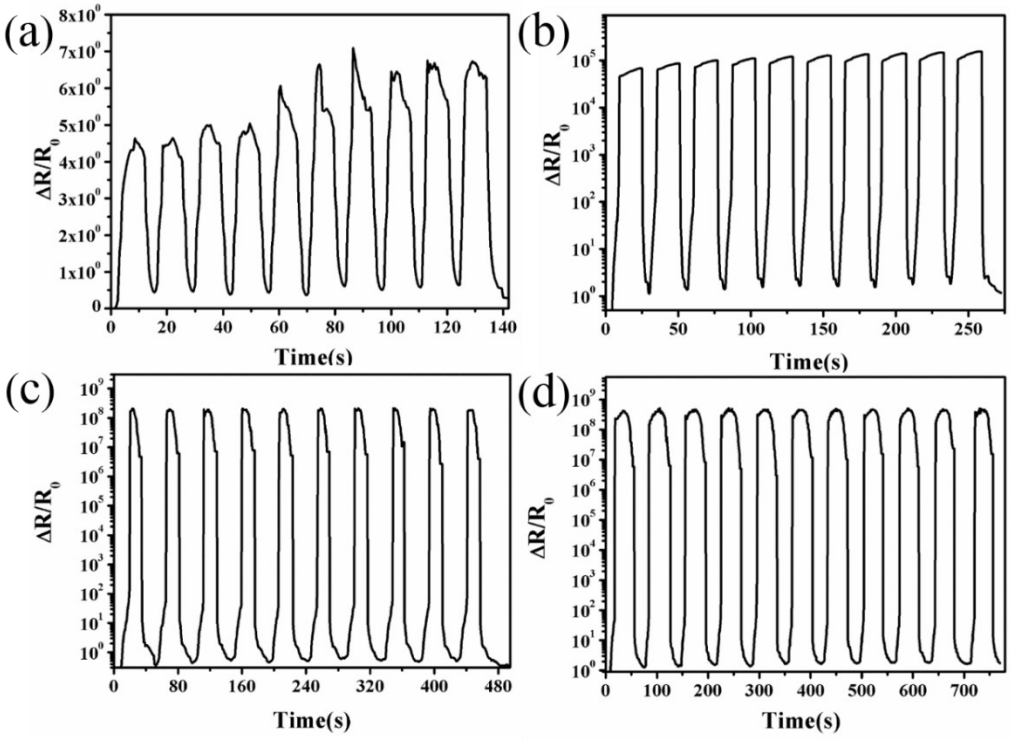

Fig. S11 $\Delta R/R_0$ versus time during the stretching–releasing cycles under different strains (a) 30%, (b) 55%, (c)100%, and (d)150%.

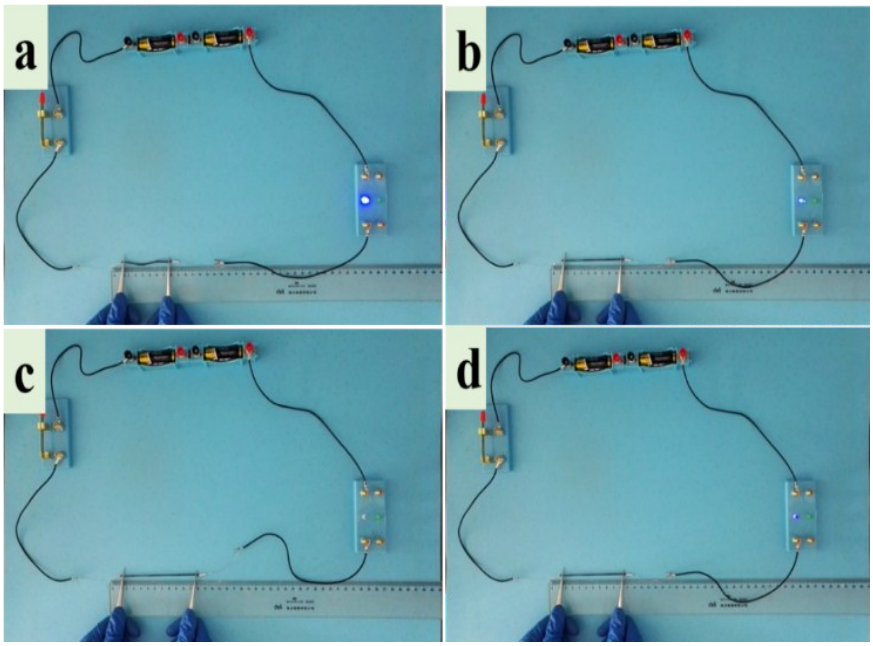

Fig. S12 The corresponding illuminated and extinct state of the LED bulb with the RB/PDA/AgNPs-90/PFDT as the conector under different strains (a) 0, (b) 22%, (c) 55% and (d) 33%.

Table S1: Some parameters for flexible strain sensors extracted from literatures and our work

Matrix	Conductive fillers	Maxi strain	Gauge factor	Reference and year
Styrene-butadiene-styrene (SBS)	FGS, AgNPs	680%	~10^7	2017[1]
Elastic tape	Graphene layer	82%	150	2016[2]
Polydimethylsiloxane (PDMS)	AgNPs	20%	2.05	2014[3]
Polydimethylsiloxane (PDMS)	Graphene platelets	20%	27.7~164.5	2016[5]
Thermoplastic urethane (TPU)	Graphene/AgNPs	1000%	476	2016[7]
Polydimethylsiloxane (PDMS)	SWCNT	280%	0.82	2011[8]
Polydimethylsiloxane (PDMS)	AgNWs	70%	2~14	2014[11]
Polydimethylsiloxane (PDMS)	Graphene	30%	98.66	2016[12]
Rubber	Graphene	800%	35	2014[13]
Thermoplastic urethane (TPU)	CB, MWNTs	200%	5~140238	2013[14]
Pen-on-paper	Graphite	0.62%	536.6	2015[16]
Rubber band	AgNPs	>1000%	~10^8	This work